Available online at www.sciencedirect.com
SCIENCE DIRECT®
Peptides 24 (2003) 1795–1805
PEPTIDES
www.elsevier.com/locate/peptides

Quantitative interactions between cryptdin-4 amino terminal variants and membranes

Donald P. Satchell[a,1], Tanya Sheynis[b], Sofiya Kolusheva[b], Jason Cummings[c], T. Kyle Vanderlick[c], Raz Jelinek[b], Michael E. Selsted[a,d], Andre J. Ouellette[a,d,*]

[a] *Department of Pathology, College of Medicine, University of California, Irvine, CA 92697-4800, USA*
[b] *Department of Chemistry, Ben-Gurion, University of the Negev, Beersheva, Israel*
[c] *Department of Chemical Engineering, Princeton University, Princeton, NJ 08544, USA*
[d] *Department of Microbiology and Molecular Genetics, College of Medicine, University of California, Irvine, CA 92697-4800, USA*

Received 3 April 2003; accepted 1 August 2003

Abstract

Paneth cells secrete α-defensins into the lumen from the base of small intestinal crypts, and cryptdin-4 (Crp4) is the most potent mouse α-defensin in vitro. Purified recombinant Crp4 and Crp4 variants with (des-Gly)-, (Gly1Val)-, (Gly1Asp)-, and (Gly1Arg)-substitutions were all bactericidal with Crp4 and (Gly1Arg)-Crp4 being slightly more active than other variants. Bactericidal activities correlated directly with permeabilization of live *Escherichia coli*, with equilibrium binding to *E. coli* membrane phospholipid bilayers and vesicles, and with induced graded fluorophore leakage from phospholipid vesicles. The Crp4 peptide N-terminus affects bactericidal activity modestly, apparently by influencing peptide binding to phospholipid bilayers and subsequent permeabilization of target cell membranes.

Keywords: Innate immunity; Paneth cells; Polymerase chain reaction; Recombinant peptide expression; α-Defensin; Reverse-phase high performance liquid chromatography; Matrix-assisted laser desorption time-of-flight mass spectrometry; Surface plasmon resonance; Lipid polydiacetylene vesicles; ANTS-DPX leakage; Antimicrobial peptide

1. Introduction

Paneth cells reside at the base of the crypts of Lieberkühn in the small intestine, where they secrete large, apically oriented granules that contain high levels of antimicrobial peptides and proteins, including lysozyme [7,26,37], secretory phospholipase A_2 [20], and α-defensins [4,21,25,27]. Paneth cells discharge these granules in response to cholinergic stimulation or when exposed to bacteria or bacterial antigens [2,29,30]. α-Defensins are 3–4 kDa bactericidal peptides that are cationic, amphipathic, and have a defining tridisulfide arrangement and β-sheet polypeptide backbone [9,17,32]. Mouse α-defensins, termed cryptdins, account for ∼70% of the bactericidal peptide activity in Paneth cell secretions [2].

Cryptdins are components of mouse innate enteric immunity in vivo as shown by studies of mice lacking a key processing enzyme in the biosynthetic pathway [40]. Matrix metalloproteinase-7 (MMP-7, matrilysin, EC 3.4.24.23) is the enzyme responsible for processing and activation of mouse Paneth cell procryptdins [1,40]. Paneth cells of MMP-7-null mice contain high levels of cryptdin precursors but produce no detectable functional cryptdin peptides [1,40]. This deficiency correlates with defective clearing of orally administered bacteria, and MMP-7 knockouts are ∼10-fold more susceptible to systemic disease when infected orally with virulent *Salmonella enterica* serovar typhimurium (*S. typhimurium)* [40]. Thus, studies that elucidate mechanisms of peptide action contribute to the understanding of innate immunity in molecular terms.

Studies of certain human and mouse α-defensins implicate the peptide N-terminus as a determinant of bactericidal activity [6]. For example, the human neutrophil α-defensins HNP-1, -2 and -3 are identical except at their N-termini, where HNP-1 terminates as ACYCR . . . , HNP-2 as CYCR . . . , and HNP-3 as DCYCR . . . [6]. In the context of the HNP-1/3 polypeptide backbone, HNP-1 and HNP-3 are variants of HNP-2 with Ala and Asp at their respective N-termini, and those modifications strongly influence peptide activities. For example, HNP-1 and HNP-2 possess nearly equivalent broad-spectrum microbicidal activities, but the activity of HNP-3 is severely attenuated against

* Corresponding author. Tel.: +1-949-824-2662; fax: +1-949-824-1098.
E-mail address: aouellet@uci.edu (A.J. Ouellette).
[1] Present address: The Dow Chemical Company, Biocides R&D, Buffalo Grove, IL 60089, USA.

0196-9781/$ – see front matter © 2003 Elsevier Inc. All rights reserved.
doi:10.1016/j.peptides.2003.08.020

certain microorganisms [6]. HNP-3 is 14-fold less bactericidal against *Staphylococcus aureus* 502a, and it has only ∼1% the activity of HNP-1 and 2 against *Cryptococcus neoformans*. In mice, enteric α-defensins recovered from the small intestinal lumen included N-terminally truncated cryptdins that had reduced antimicrobial activities in in vitro assays [24]. One peptide in particular, (des-Gly)-Crp4, was lacking the Gly residue from the Crp4 peptide N-terminus and exhibited less bactericidal activity against certain Gram-negative bacteria, suggesting that the Crp4 N-terminus was a determinant of microbicidal activity.

In this report, amino acid substitutions were introduced to alter the charge and hydrophobicity of the Crp4 N-terminus, and the variant peptides were tested for differences in microbicidal activity. Compared to naturally existing HNP-1/3, changes to the N-terminal charge and hydrophobicity of Crp4 altered microbicidal activity only modestly. Nevertheless, the small differences in bactericidal activity of the N-terminal Crp4 variants correlated with quantitative effects on peptide–membrane interactions and with the kinetics and extent of peptide-induced cellular and vesicular permeabilization events.

2. Method

2.1. Preparation of recombinant Crp4 peptides

Recombinant Crp4 peptides were expressed in *Escherichia coli* as N-terminal 6X-histidine tagged fusion proteins. DNA coding for the Crp4 peptide, corresponding to nucleotides 182–274 of mouse Crp4 cDNA [22], was amplified and directionally subcloned into the *Eco*RI and *Sal*I sites of the pET28a expression vector (Novagen, Inc., Madison, WI, USA). The Crp4 coding cDNA sequences were amplified using forward primer [ER1-Met-C4-F] 5′-GCGCG AATTC ATCGA GGGAA GGATG GGT TTGTT ATGCT ATTGT, paired with reverse primer, [pMALCrp4-R]. To introduce substitutions at the N-terminus, the common reverse primer [pMALCrp4-R] 5′-ATATA TGTCG ACTCA GCGAC AGCAG AGCGT GTACA ATAAA TG [24] was paired with the following forward primers: (des-Gly)-Crp4, [ER1-Met-XGC4-F] 5′-GCGCG AATTC ATCGA GGGAA GGATGTTG TTATG CTATT GT; (Gly1Asp)-Crp4, [ER1-Met-Gly1AspC4-F] 5′-GCGCG AATTC ATCGA GGGAA GGATG GAC TTGTT ATGCT ATTGT; (Gly1Val)-Crp4, [ER1-Met-Gly1ValC4-F] 5′-GCGCG AATTC ATCGA GGGAA GGATG GTT TTGTT ATGCT ATTGT; and (Gly1Arg)-Crp4, [ER1-Met-Gly1ArgC4-F] 5′-GCGCG AATTC ATCGA GGGAA GGATG CGCTT GTTAT GCTAT TGT. In each primer, the underlined codon in each Crp4 forward primer denotes the Met codon introduced immediately upstream of the designed peptide amino terminus to introduce a CNBr cleavage site. Following PCR amplification, samples of individual reactions were gel purified using in 2% agarose gels, and extracted using QIAEX II (Qiagen Inc., Valencia, CA, USA). Purified fragments were digested with *Eco*RI and *Sal*I, ligated into similarly digested pET28a plasmid DNA (Novagen, Inc.), and transformed into XL-1 Blue cells (Stratagene Cloning Systems, Inc., La Jolla, CA, USA). Positive recombinant clones were identified by *Eco*R1 and *Sal*1 digestion of plasmids from colonies and confirmed to have appropriate coding modifications by DNA sequencing.

Recombinant proteins were expressed in *E. coli* BL21(DE3)-CodonPlus-RIL cells (Stratagene) transformed with Crp4 cDNA constructs. Cells were grown at 37 °C to $OD_{620} = 0.9$ in Terrific Broth (TB) medium consisting of 12 g BactoTryptone (Becton Dickenson Microbiological Systems, Inc., Sparks, MD, USA), 24 g of BactoYeast Extract (Becton Dickenson), 4 ml glycerol, 900 ml H_2O, 100 ml of the following sterile phosphate buffer 0.17 M KH_2PO_4 and 0.72 M K_2HPO_4, and 70 μg/ml kanamycin. Fusion protein expression was induced by addition of 0.1 mM isopropyl-β-D-1-thiogalactopyranoside (IPTG), and bacterial cells were harvested by centrifugation after growth for 6 h at 37 °C and stored at −20 °C. Cells were lysed by resuspending the bacterial cell pellets in 6 M guanidine–HCl in 100 mM Tris–HCl (pH 8.1) followed by sonication at 70% power, 50% duty cycle for 2 min using a Branson Sonifier 450. Lysates were clarified by centrifugation in a Sorvall SA-600 rotor at 30,000 × *g* for 30 min at 4 °C prior to protein purification.

2.2. Purification of recombinant Crp4 proteins

His-tagged Crp4 fusion peptides were purified using nickel-nitrilotriacetic acid (Ni-NTA, Qiagen) resin affinity chromatography [36]. Cell lysates were incubated with Ni-NTA resin at a ratio of 25:1 (v/v) in 6 M guanidine–HCl, 20 mM Tris–HCl (pH 8.1) for 4 h at 4 °C. Fusion proteins were eluted with 2 column volume of 6 M guanidine–HCl, 1 M imidazole, 20 mM Tris–HCl (pH 6.4), dialyzed in SpectraPor 3 (Spectrum Laboratories, Inc., Rancho Dominguez, CA, USA) membranes against 5% acetic acid and lyophilized. The Met residue added to the N-terminus of each Crp4 peptide provided a cyanogen bromide (CNBr) cleavage site in the His-tagged fusion peptide. CNBr cleavage was performed on lyophilized His-Crp4 peptide dissolved in 50% formic acid to which solid CNBr was added to a final concentration of 10 mg/ml, and the mixtures were incubated for 8 h in foil wrapped polypropylene tubes at 25 °C. The cleavage reactions were terminated by addition of 10 volumes of H_2O, followed by freezing and lyophilization of the peptide mixture. Cleaved peptide samples were then dissolved in 5% acetic acid and stored at 4 °C.

The Crp4 peptides were purified to homogeneity using reverse-phase high performance liquid chromatography (RP-HPLC). After CNBr cleavage, Crp4 peptides were separated from the 36 amino acid 6X-His-tag fusion partner by C-4 RP-HPLC on a Vydac 214TP1010 column (Grace Vydac, Hesperia, CA, USA). Protein samples were applied

to C-4 columns in aqueous 0.1% trifluoroacetic acid (TFA) and resolved using a 55 min gradient of 0 to 35% acetonitrile. Crp4 peptides were purified to homogeneity by analytical C-18 RP-HPLC on a Vydac 218TP54 column. Using the same mobile phase, each Crp4 variant was resolved with elution times ranging from 21 to 24 min using a 55 min, 10–45% acetonitrile gradient. Protein fractions containing Crp4 were identified by acid-urea polyacrylamide gel electrophoresis (AU-PAGE) as described [23,33,35] to confirm comigration with natural Crp4 and to evaluate the homogeneity of the preparation. Peptide concentrations were quantitated by amino acid analysis (Waters Alliance, Bedford, MA, USA) or UV absorption spectrophotometry at 280 nm ($\in = 3355\,M^{-1}\,cm^{-1}$). Molecular masses of purified peptides were determined using matrix-assisted laser desorption ionization mode mass spectrometry (Voyager-DE MALDI-TOF, PE-Biosystems, Foster City, CA, USA) in the UCI Biomedical Protein and Mass Spectrometry Resource Facility.

2.3. Microbicidal assays

Recombinant peptides were tested for microbicidal activity against *E. coli* ML35, *S. typhimurium* (*PhoP-*), *Vibrio cholera*, *S. aureus* 710a, *Listeria monocytogenes* 104035, *C. neoformans* 271a and *C. albicans* as previously described [16]. Exponential-phase bacteria or fungi, respectively, grown in trypticase soy broth (TSB) or Sabouraud dextrose broth (SDB) at 37 °C, were deposited by centrifugation at 1700 × *g* for 10 min, washed in 10 mM PIPES (pH 7.4), and resuspended in 10 mM PIPES (pH 7.4) supplemented with 0.01 volumes of TSB or SDB. Peptide samples were lyophilized and dissolved in 10 mM PIPES (pH 7.4) at 1 mg/ml. Approximately 1×10^6 microorganisms were incubated with test peptides in a total volume of 50 μl for 1 h (bacteria) or 2 h (fungi) in a shaking incubator at 37 °C. Following incubation, 20 μl samples of incubation mixtures were diluted 1:2000 with 10 mM PIPES (pH 7.4) and 50 μl of the diluted samples were plated on TSB or SDB agar plates using an Autoplate 4000 (Spiral Biotech Inc., Bethesda, MD, USA). Surviving microorganisms were quantified as colony forming units per milliliter (CFU/ml) after incubation at 37 °C for 12 to 18 h.

2.4. Permeabilization of E. coli cell membranes

The relative ability of Crp4 peptides to permeabilize *E. coli* cell cytoplasmic membrane was assayed by measuring hydrolysis of *o*-nitrophenyl-β-D-galactopyranoside (ONPG) by cytoplasmic β-galactosidase and colorimetric detection of the ONPG hydrolysis product *o*-nitrophenol [16]. In lactose permease-deficient and β-galactosidase-constitutive *E. coli* ML35 cells [15], peptide-induced membrane disruption allows the ONPG substrate to diffuse into the bacterial cell for hydrolysis by cytoplasmic β-galactosidase [19]. To measure Crp4-induced ONPG conversion in *E. coli* ML35, 158 μl of substrate buffer consisting of 10 mM PIPES (pH 7.4), 1% (v/v) TSB and 10 mM ONPG was combined with 2 μl of peptides, as noted the legend to Fig. 6, and 40 μl of log-phase *E. coli* ML35 cells ($OD_{620} = 0.1$) in 10 mM PIPES (pH 7.4), 1% TSB. The kinetics of ONP production at 37 °C was measured by absorbance at 400 nm for 120 min using a 96-well Spectra Max plate spectrophotometer (Molecular Devices Corp., Sunnyvale, CA, USA). The maximum velocity of ONPG hydrolysis (V_P) reflects the concentration-dependent, maximum rate of ONPG diffusion into the bacterial cytoplasm following membrane perturbation. V_P was calculated by non-linear regression of the time course of ONP absorbance at 400 nm [19] using the first order kinetic equation of Hill

$$\left[Y = \frac{AX^B}{C^B + X^B} \right] \quad (1)$$

The maximum rate of hydrolysis and the corresponding time points were determined using the first differential of Eq. (1),

$$\left[\frac{dY}{dX} = \frac{AB(X^{B-1})}{C^B + X^B} \left(1 - \left(\frac{X^B}{C^B + X^B} \right) \right) \right] \quad (2)$$

with coefficients derived from the kinetic data for ONPG hydrolysis fit with Eq. (1) using SigmaPlot (SPSS Science, Chicago, IL, USA). The variables are defined as follows: (*Y*) measured absorbance of ONP at 400 nm, (*X*) time interval corresponding to (*Y*) in minutes and decimal seconds, (*A*) the maximum ONP absorbance value, (*B*) concentration-dependent cooperativity for ONPG hydrolysis determined using Eq. (1), and (*C*) the corresponding time point to attain 50% of the absorbance maximum (*A*).

2.5. Binding of Crp4 peptides to phospholipid bilayers

Surface plasmon resonance (SPR) was used to determine the equilibrium binding constant (K_d) of Crp4 and each peptide variant to *E. coli* phospholipids on a Biacore 3000 instrument (Biacore International AB, Uppsala, Sweden). large unilamellar vesicles (LUV) were prepared from whole cell phospholipids extracted from *E. coli* (Sigma–Aldrich, St. Louis, MO, USA). The lipid mixture was dissolved in methylene chloride with gentle mixing until clear and homogeneous and then dried under a stream of N_2 gas, frozen, and lyophilized for 3 h to remove residual methylene chloride. The dried lipid cake was suspended in 1 ml 10 mM PIPES (pH 7.4, Fluka, Sigma–Aldrich, Milwaukee, WI, USA), and used to make LUV by repeated extrusion of the lipid suspension through an extruder fitted with polycarbonate membranes with 0.1 μm pores (Avanti Polar Lipids, Inc., Alabaster, AL, USA). The Biacore L1 sensor chip surface was conditioned by injection of 100 μl 40 mM octyl-D-glucoside (Pierce Chemical Company, Inc., Rockford, IL, USA) in 10 mM PIPES (pH 7.4) at a flow rate of 10 μl/min, followed by injection of 100 μl LUV (2 μl/min) consisting of 5.8 mM total lipid. The resulting lipid bilayer

was stable as judged by the consistency of SPR signals after repeated injection of 0.10 M NaOH [5,11]. Injections of 0.5 μg/ml bovine serum albumin (Sigma), showed ≤70 relative response units of binding to the sensor surface in the presence of the lipid bilayer, evidence of phospholipid coverage of the sensor surface.

Equilibrium binding of Crp4 peptides to the phospholipid surface was performed by injection of 0–10 μM Crp4 peptide solutions in 10 mM PIPES (pH 7.4) at a flow rate of 30 μl/min at 37 °C. SPR signals were monitored for 15 min after injection to record both the association and dissociation kinetics of the peptide–phospholipid bilayer interaction. At all concentrations assayed, peptide binding reached equilibrium within 120 s, and peptide dissociation was monitored for 10 min following the injection. After each injection period, bilayers were washed with 30 μl 0.5 M KCl at a flow rate of 10 μl/min, and desorption of Crp4 was judged by the return of SPR signals to pre-peptide injection values. Equilibrium binding constants (K_d) for peptide affinity to the phospholipid bilayer were determined by non-linear regression using the Marquardt–Levenberg algorithm of the protein binding isotherm in the program SigmaPlot.

2.6. Peptide interactions with lipid/polydiacetylene (PDA) mixed vesicles

Colorimetric lipid/PDA vesicles were prepared using dimyristoylphosphatidylcholine (DMPC) and dimyristoylphosphatidylglycerol (DMPG) purchased from Sigma–Aldrich Co. Total lipids were extracted from *E. coli* B/r H-266, grown at 37 °C for 24 h in LB medium. Bacteria deposited by centrifugation were resuspended in 4 M NaCl and an equal volume of a 1:1 mixture of chloroform and methanol. After the mixture was shaken gently for 1 h and refrigerated overnight, the chloroform and aqueous phases were separated by centrifugation at 5000 × *g* for 15 min, and the aqueous methanol solution was re-extracted with chloroform. The combined chloroform extracts were concentrated by evaporation, and the residual lipid-containing fraction was lyophilized. Lipids were stored at −20 °C.

The diacetylenic monomer, 10,12-tricosadiynoic acid (GFS Chemicals, Powell, OH, USA), was washed in chloroform, and filtered through a 0.45 μm filter prior to use. Vesicles consisting of defined lipid/PDA (2:3 molar ratio) or using total cell lipids extracted from *E. coli* at 2:3 mass ratio of total lipid to PDA were prepared as follows. All lipid constituents were dissolved in chloroform/ethanol (1:1), dried together in vacuo to constant weight, and suspended in deionized water by probe sonication at 70 °C for 2–3 min. The vesicle suspension was cooled to room temperature, incubated overnight at 4 °C, and polymerized by irradiation at 254 nm for 10–20 s, resulting in solutions having an intense blue appearance. Crp4, (des-Gly)-Crp4, and (Gly1Arg)-Crp4, at concentrations ranging from 0.2 to 20 μM, were added to 60 μl vesicle solutions consisting of 0.5 mM total lipid in 25 mM Tris–HCl (pH 8). Following addition of the peptides, the solutions were diluted to 1 ml and spectra were acquired at 28 °C between 400 and 700 nm on a Jasco V-550 spectrophotometer (Jasco Corp., Tokyo), using a 1 cm optical path cell. Blue-to-red color transitions within the vesicle solutions, defined as the colorimetric response (percent CR), were calculated as follows [13,28]: percent $CR = [(PB_0 - PB_I)/PB_0] \times 100$, where $PB = A_{blue}/(A_{blue} + A_{red})$, and A is the absorbance at 640 nm, the "blue" component of the spectrum, or at 500 nm, the "red" component. The terms "blue" and "red" refer to the visual appearance of the vesicle solutions, not actual absorbancies. PB_0 is the blue/red ratio of the control sample before induction of a color change, and PB_I is the value obtained for the vesicle solution after the colorimetric transition occurred.

2.7. Fluorescence-based vesicle leakage assays of peptide–membrane interactions

Crp4, (des-Gly)-Crp4, and (Gly1Arg)-Crp4 also were tested for their relative abilities to induce leakage from large unilamellar vesicles of defined composition. For these studies, unilamellar phospholipid vesicles of palmitoyl–oleoyl–phosphatidyl glycerol (POPG) or of 80% POPG and 20% palmitoyl–oleoyl–phosphatidyl choline (POPC) were prepared and loaded with the ANTS/DPX fluorophore/quencher system [38]. Lipids were purchased from Avanti Polar Lipids (Birmingham, AL, USA) and ANTS/DPX from Molecular Probes (Eugene, OR, USA). Briefly, aqueous lipid solutions consisting of 17 mM ANTS, 60.5 mM DPX, 10 mM HEPES, 31 mM NaCl, and 19.5 mM NaOH (solution osmolarity 260 mOsm, pH 7.4) were vortexed, frozen, and thawed for five cycles and then extruded through polycarbonate filters of 100 nm pore size. Vesicles were separated from unencapsulated ANTS/DPX by passing the solution through a Sephadex G-50 medium resin column, using as the eluant a solution consisting of 130 mM NaCl, 10 mM HEPES, and 4.5 mM NaOH (260 mOsm, pH 7.4). Vesicular suspensions were diluted with this same solution to a final value of approximately 74 μM total lipid and were then incubated with peptide at ambient temperature. Time-dependent fluorescence, produced by ANTS release, was monitored at 520 nm (excitation at 353 nm [28]). Kinetics of the leakage response was a function of peptide concentration. However, equilibrium was attained well before 4 h. Thus, the 4 h value was plotted as a function of peptide concentration, normalized to the fluorescence obtained when vesicles were solubilized with Triton X-100.

3. Results

3.1. Production of recombinant Crp4 peptides

Efficient recombinant expression of Crp4 and Crp4 variants was obtained in *E. coli* using pET-28a (Section 2), providing improved yields compared to those reported pre-

		Theoretical M.W.	Experimental M.W.
Cryptdin-4	GLLCYCRKGHCKRGERVRGTCGIRFLYCCPRR	3755.5	3756
(des-Gly)-Cryptdin-4	LLCYCRKGHCKRGERVRGTCGIRFLYCCPRR	3698.5	3700
(G1D)-Cryptdin-4	DLLCYCRKGHCKRGERVRGTCGIRFLYCCPRR	3813.6	3814
(G1V)-Cryptdin-4	VLLCYCRKGHCKRGERVRGTCGIRFLYCCPRR	3797.6	3798
(G1R)-Cryptdin-4	RLLCYCRKGHCKRGERVRGTCGIRFLYCCPRR	3854.6	3854

Fig. 1. Biochemical composition of the recombinant Crp4 peptides. Crp4 and N-terminal variants are shown in alignment. Theoretical and experimentally determined peptide molecular weights are reported for each Crp4 amino acid sequence. The conserved α-defensin intramolecular disulfide bond arrangement is identified by the connecting bars above the peptide sequences. Net charge was calculated based on the pK_a of ionizable side chains at pH 7.4 present in the peptide sequences.

viously [24]. Recombinant 6x-His-Crp4 fusion peptides purified by affinity chromatography from bacterial cell lysates (Section 2) were cleaved with CNBr to release Crp4 peptides from the fusion partner free of ancillary residues [28,36]. The molecular masses of individual recombinant peptides matched their theoretical values by MALDI-TOF mass spectrometry (Fig. 1), and peptide homogeneity was confirmed using analytical RP-HPLC (not shown) and by AU-PAGE (Fig. 2). All Crp4 peptide variants were homogeneous by these criteria, and each migrated in AU-PAGE as expected, based net charge relative to Crp4 [31]. Thus, the expressed and purified Crp4 peptides were biochemically equivalent to natural Crp4, or as predicted from the modifications at their N-termini.

3.2. Bactericidal activities of the Crp4 variants

Crp4 and Crp4 N-terminal variants were nearly indistinguishable in their ability to kill Gram-negative and Gram-positive bacteria. Because the microbicidal activities of human neutrophil α-defensins improve when nutrients are added to assay mixtures [6,34], Crp4 peptides also were assayed with nutrient supplementation. Under these new conditions, the sensitivity and reproducibility of Crp4 microbicidal activity was markedly enhanced relative to our previous antimicrobial assays of Crp4 and (des-Gly)-Crp4 in 10 mM PIPES (pH 7.4) [22,23]. As noted in Section 4, the robust concentration-dependent activity of Crp4 and all peptide variants (Figs. 3 and 5) eliminated the previously observed attenuation of (des-Gly)-Crp4 activity. Against *E. coli*, *S. typhimurium PhoP*, and *V. cholera*, Crp4 and (Gly1Arg)-Crp4 consistently showed slightly greater activity than the remaining peptides assayed, killing 99.9% of exposed bacteria between 2.5 and 10 μg/ml (Fig. 3A–C). On the other hand, (Gly1Asp)-Crp4 had somewhat lower activity against Gram-negative species, requiring two to four times more peptide to kill at the level of Crp4 (Fig. 3A–C). Thus, compared to the effects of the N-terminal Asp on HNP-3 activity [6], the Gly1Asp substitution caused negligible attenuation of bactericidal activity. (Gly1Val)-Crp4 also displayed diminished activity against certain target cells, suggesting that the decreased activity is not attributable solely to N-terminal charge. Although subtle differences in the concentration dependence of bacterial cell killing were observed, *S. aureus* and *L. monocytogenes* were killed by all Crp4 peptides at concentrations of 10–20 μg/ml (Fig. 4A and B). *L. monocytogenes* was most sensitive to (Gly1Arg)-Crp4 and Crp4, and (Gly1Asp)-Crp4 was slightly less active against *S. aureus* and *L. monocytogenes* (Fig. 4A and B), consistent with the previously observed preferential killing of Gram-negative bacteria. However, unlike the profound attenuating effects of electronegative substitution at HNP N-termini [17], the Crp4 variants that differed most in microbicidal activity varied only by a factor of two to three-fold (Fig. 3).

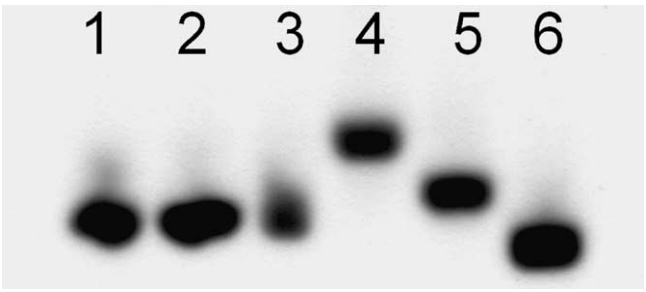

Fig. 2. Purified recombinant Crp4 peptides. Expressed Crp4 peptides were purified using NTA affinity chromatography, C-4 and C-18 reverse-phase HPLC. The retention times of individual Crp4 variants were very similar. Purified peptides were evaluated for homogeneity using non-reducing AU-PAGE and mass spectrometry. The high sensitivity of AU-PAGE to slight differences in net positive charge relative to size enables the resolution of Crp4 variant peptides. Coomassie blue stained AU-PAGE; 4 μg of each purified peptide was loaded into each lane. Lanes: 1, native Crp4; 2, Crp4; 3, (des-Gly)-Crp4; 4, (Gly1Asp)-Crp4; 5, (Gly1Val)-Crp4; 6, (Gly1Arg)-Crp4.

3.3. Microbicidal activity of the Crp4 variants against fungi

The opportunistic fungi *C. neoformans* and *Candida albicans* were less sensitive than bacteria to the microbicidal effects of Crp4 and N-terminal Crp4 variants (Fig. 5). *C. neoformans* was more susceptible than *C. albicans*, which was insensitive to (Gly1Val)-, (Gly1Asp)-, and (des-Gly)-Crp4 exposure and only slightly affected by Crp4 or (Gly1Arg)-Crp4 (Fig. 5B). Consistent with their bactericidal activities (Figs. 3 and 4), Crp4 and (Gly1Arg)-Crp4 were slightly more active against both fungi than the other Crp4 variants (Fig. 5A).

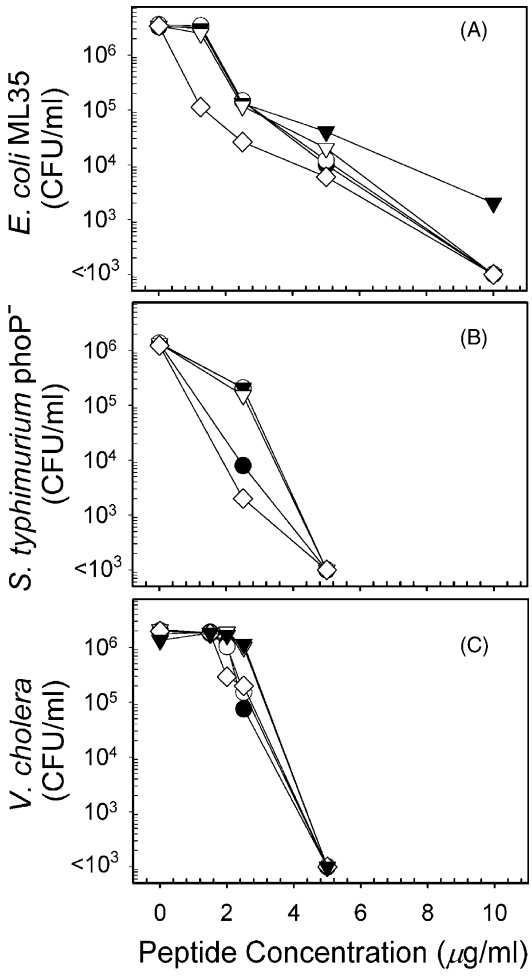

Fig. 3. Bactericidal activity of recombinant Crp4 peptides against Gram-negative bacteria. Exponentially growing *E. coli* ML35 (A), *S. typhimurium* (*PhoP*) (B), or *V. cholera* (C) were exposed to increasing concentrations of Crp4 peptide in 10 mM PIPES pH 7.4 buffer, 1% TSB for 1 h at 37 °C (Section 2). Following exposure, bacteria were plated onto TSA plates and incubated for 16 h at 37 °C. Surviving bacteria were quantified and the results are reported as the number of colony forming units per milliliter (CFU/ml) for each peptide concentration. Bacterial counts below 1×10^3 CFU/ml indicate no surviving colonies on the incubated plate. Symbols: (●) Crp4, (○) (des-Gly)-Crp4, (▼) (Gly1Asp)-Crp4, (▽) (Gly1Val)-Crp4, (◇) (Gly1Arg)-Crp4.

3.4. Permeabilization of *E. coli* by Crp4 peptides

To determine whether modifications of N-terminal net charge and hydrophobicity modulated the ability of Crp4 to permeabilize the inner bacterial cell membrane, cell permeabilization experiments were performed against *E. coli* ML35 (Fig. 6; Section 2). Permeabilization of *E. coli* by the Crp4 peptides was concentration-dependent and corresponded with the relative bactericidal activities of the peptides. At concentrations ≥2.3 μM (8.5–8.9 μg/ml), all Crp4 N-terminal variants killed 99.9% of exposed *E. coli* ML35 cells (Fig. 3A), and each peptide permeabilized *E. coli* equivalently at concentrations of 2.3 μM or greater (Fig. 6A–C; Table 1). On the other hand, at ≤2.3 μM peptide, the rate and

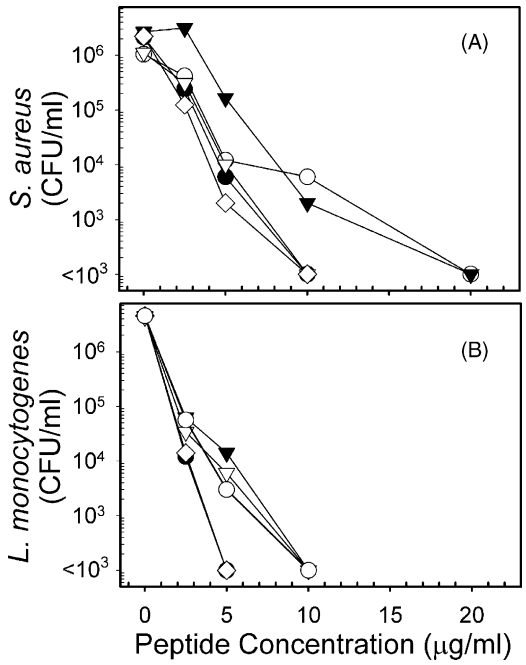

Fig. 4. Bactericidal activity of Crp4 peptides against Gram-positive bacteria. Exponentially- growing *S. aureus* 710a or *L. monocytogenes* 104035 were exposed to increasing concentrations of the Crp4 peptides. All assay parameters were performed as described in Fig. 3. Symbols: (●) Crp4, (○) (des-Gly)-Crp4, (▼) (Gly1Asp)-Crp4, (▽) (Gly1Val)-Crp4, (◇) (Gly1Arg)-Crp4.

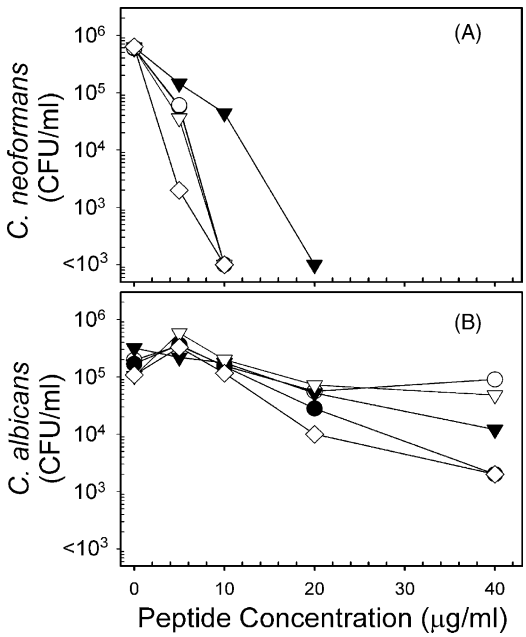

Fig. 5. Fungicidal activity of Crp4 peptides. Yeast-like fungi, *C. neoformans* (A) 271a and *C. albicans* (B) were grown to mid-log phase and exposed to increasing concentrations of Crp4 peptides in 10 mM PIPES (pH 7.4), 1% SAB for 2 h at 37 °C. Following peptide exposure, fungi were plated onto SAB plates and incubated for 36 h at 37 °C (Section 2). Surviving fungi were quantified as described in Fig. 3. Symbols: (●) Crp4, (○) (des-Gly)-Crp4, (▼) (Gly1Asp)-Crp4, (▽) (Gly1Val)-Crp4, (◇) (Gly1Arg)-Crp4.

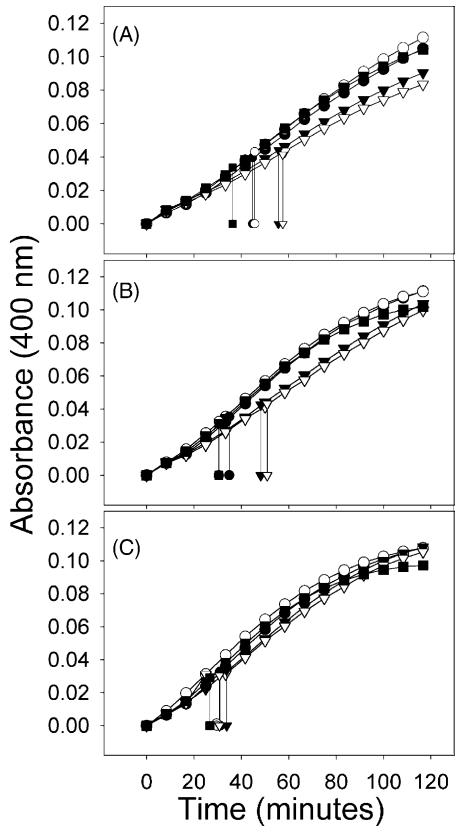

Fig. 6. Permeabilization of the *E. coli* cytoplasmic membrane by Crp4 N-terminal variants. The kinetics for membrane permeabilization by Crp4 peptides was determined by monitoring the rate of *o*-nitrophenyl-α-D-galactopyranoside (ONPG) hydrolysis by cytoplasmic β-galactosidase in *E. coli* ML35. ONPG hydrolysis was measured following addition of Crp4 peptide (A400 nm at 5 s intervals for 120 min, 37 °C). The maximum velocity of enzyme catalyzed ONPG hydrolysis (V_P) was determined by non-linear regression for each time course (Section 2). The time required to reach V_P were compared by determining the time at which the maximum rate of hydrolysis was reached (Section 2), indicated by the vertical line intersecting each kinetic curve (defined as T_P). Values for V_P and T_P are listed in Table 1. Peptide concentrations were as follows: (A) 1.0 μM; (B) 1.5 μM; (C), 2.3 μM. Symbols: (●) Crp4, (○) (des-Gly)-Crp4, (▼) (Gly1Asp)-Crp4, (▽) (Gly1Val)-Crp4, (◇) (Gly1Arg)-Crp4. For each panel, V_P and T_P values represent the mean from triplicate determinations for each peptide.

magnitude of *E. coli* cell permeabilization correlated with the bactericidal activities of individual peptides against *E. coli* (Figs. 3A and 6), with (Gly1Arg)-Crp4, Crp4, and (des-Gly)-Crp4 inducing ONPG hydrolysis more rapidly and to a greater extent than (Gly1Asp)- and (Gly1Val)-Crp4 (Fig. 6). The reduced level of ONPG hydrolysis and increased time needed for (Gly1Asp)-Crp4 and (Gly1Val)-Crp4 to reach their respective V_P values (Fig. 6) is consistent with their lower bactericidal activities against *E. coli* (Fig. 3A). When *E. coli* ML35 cells were exposed to 1.5 μM Crp4, only 20–30 min exposures were required to kill >99.9% of the exposed cells, but 45–60 min exposures were needed to attain comparable killing with 1.5 μM (Gly1Val)-Crp4 (data not shown). Because the permeabilization of live *E. coli* by N-terminal Crp4 variants correlated with the killing activities of the peptides against this organism (Fig. 3A–C; Table 1), three approaches were used to test whether the relative bactericidal activity of individual peptides corresponded with quantitative peptide–membrane interactions.

3.5. Binding of Crp4 peptides to *E. coli* phospholipids

The equilibrium-binding constants (K_d) of Crp4 peptides to *E. coli* phospholipid bilayers were determined by surface plasmon resonance (SPR) on Biacore L-1 sensor chip treated with large unilamellar vesicles composed of *E. coli* extracted phospholipids [5]. Binding experiments were performed at 0.267–10 μM peptide concentration, i.e. 1–37.5 μg/ml Crp4, the range over which the peptides were microbicidal against *E. coli* (Fig. 3). A representative ligand binding isotherm and nonlinear regression for Crp4 binding is shown in Fig. 7, and the K_d of individual peptides are summarized in Table 2. The respective affinities of Crp4 and its variants for the *E. coli* phospholipid bilayer agrees well with their relative bactericidal activities. Because SPR only distinguishes changes in quantity of bound peptide [5,11], possible reorganization or reorientation of peptides into higher ordered structures within the bilayer could not be analyzed by this approach [3,10,39], and so comparative peptide–phospholipid interactions were evaluated in two additional model membrane systems.

Table 1
E. coli membrane permeabilization by Crp4 and the N-terminal variants.

Peptide concentration (μM)	Crp4		(des-Gly)-Crp4		(Gly1Val)-Crp4		(Gly1Asp)-Crp4		(Gly1Arg)-Crp4	
	V_P	T_P	V_P	T_P	V_P	T_P	V_P	T_P	V_P	T_P
1.0	79.5	44.7	82.3	45.7	62.1	55.6	58.5	57.5	82.8	36.3
1.5	101.2	34.2	101.5	30.4	74.2	48.2	71.0	50.8	104.5	30.4
2.3	108.9	30.9	106.5	29.5	95.0	33.8	89.1	30.7	116.7	26.7
3.5	107.5	26.5	105.5	25.5	109.2	26.2	103.2	25.7	115.3	20.4

The maximum velocity of enzyme catalyzed ONPG hydrolysis (V_P in pmol/min) following permeabilization of the *E. coli* cytoplasmic membrane and the time to achieve V_P (T_P in minutes) are listed for each peptide. V_P and T_P were determined as described in Fig. 4.

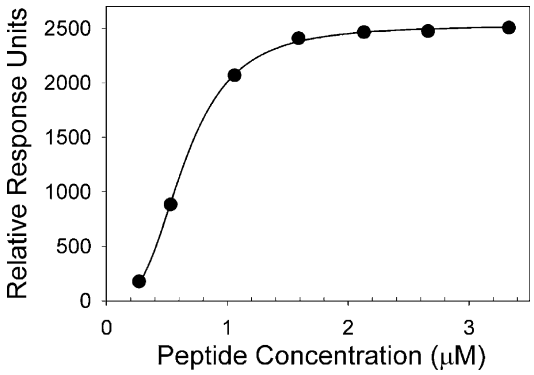

Fig. 7. Equilibrium binding isotherm of Crp4 binding to an *E. coli* phospholipid bilayer. Large unilamellar vesicles composed of *E. coli* phospholipids were used to establish a phospholipid bilayer on a Biacore L1 sensor chip (Section 2). Equilibrium binding of Crp4 to the phospholipid bilayer was determined by independent injections of Crp4 in 10 mM PIPES (pH 7.4) at 37 °C over a 120 s injection period. Dissociation constants were determined by non-linear regression of the binding isotherm for each Crp4 peptide and are listed in Table 2.

3.6. Crp4 interactions with lipid/PDA mixed vesicles

Interactions between Crp4, (des-Gly)-Crp4, and (Gly1Arg)-Crp4 were studied by colorimetric assays performed using lipid/PDA mixed vesicles (Section 2). The peptide-induced blue-red chromatic transitions (percent CR) were dependent on peptide concentration and the phospholipid composition of the lipid/PDA mixed vesicles (Fig. 8), and the chromatic shifts varied with the composition of the peptide N-termini. The peptides we examined, Crp4, (des-Gly)-Crp4, and (Gly1Arg)-Crp4, were added to DMPC/PDA vesicles (Fig. 8A) and lipid/PDA mixed vesicles composed of *E. coli* whole membrane phospholipids (Fig. 8B). The percent CR curves induced by (des-Gly)-Crp4 were steeper than those of the other peptides, showing that (des-Gly)-Crp4 bound more strongly to lipid bilayer head groups than Crp4 or (Gly1Arg)-Crp4 and that it inserted less deeply into the membrane [12,14,28]. At 0.5 μM (des-Gly)-Crp4, percent CR values were 50 and 25% in DMPC/PDA and *E. coli* lipid/PDA vesicles, respectively (Fig. 8A and B). In contrast, 0.5 μM Crp4 and (Gly1Arg)-Crp4 induced percent CR values of only 10–30%, evidence of enhanced insertion of these two peptides into the hydrophobic core of the lipid bilayer [14]. The modestly lower bactericidal activity of (des-Gly)-Crp4 may result from its interactions at the lipid/water interface and less perturbation of the hydrophobic core of the membrane. Consistent with this notion, the lower slopes of the percent CR curves induced by the more active Crp4 and (Gly1Arg)-Crp4 peptides suggest that they insert more deeply into the bilayer than (des-Gly)-Crp4 and that the N-terminal Gly residue of natural Crp4 influences lipid bilayer penetration.

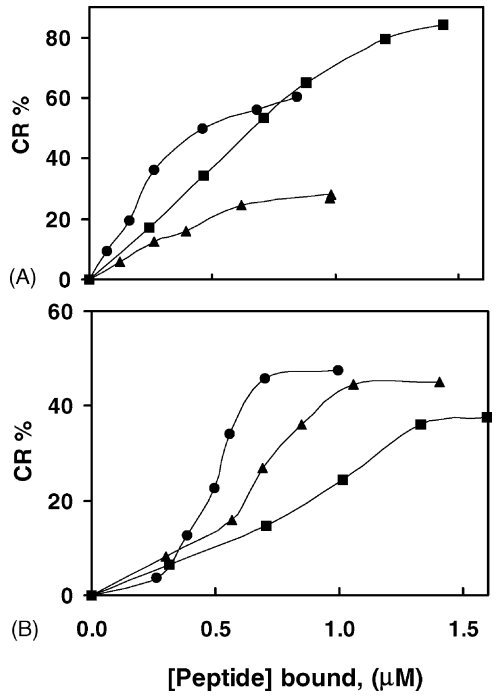

Fig. 8. Crp4 N-terminal variant interactions with lipid/PDA vesicles of differing lipid composition. PDA vesicles containing DMPC/PDA (2:3 mole ratio) (A) or total lipid extracts from *E. coli* (B) were exposed to Crp4 (■), (Gly1Arg)-Crp4 (▲), or (des-Gly)-Crp4 (●) as described in Section 2. The relative increase in percent CR is proportional to the depth of peptide insertion into the lipid bilayers. In both systems, (des-Gly)-Crp4 exhibits stronger interfacial binding to polar head groups, but Crp4 and (Gly1Arg)-Crp4 insert more deeply.

Table 2
E. coli phospholipid binding constants determined for each Crp4 peptide

Peptide	K_d (μM)	S.D.
Crp4	0.69	0.04
(des-Gly)-Crp4	0.82	0.05
(Gly1Val)-Crp4	0.77	0.09
(Gly1Asp)-Crp4	1.26	0.09
(Gly1Arg)-Crp4	0.58	0.07

Dissociation constants were determined by surface plasmon resonance as described in Fig. 5 and Section 2. Each determination was performed in triplicate.

3.7. LUV leakage studies

Interactions between membranes and peptides (Crp4, (Gly1Arg)-Crp4, (des-Gly)-Crp4) were also analyzed by examining peptide-induced leakage of low molecular weight fluorophores (ANTS) from LUV (Section 2). Results were consistent with the relative bactericidal activities of the peptides: Crp4 and (Gly1Arg)-Crp4 were more effective than (des-Gly)-Crp4; the differences were small but measurable (Fig. 9). All Crp4 peptides were more effective at inducing leakage from vesicles composed exclusively of the anionic lipid POPG (Fig. 9A) compared to LUV consisting of 80% POPG and 20% POPC (Fig. 9B), suggesting that electrostatic interactions regulate the degree of vesicle leakage.

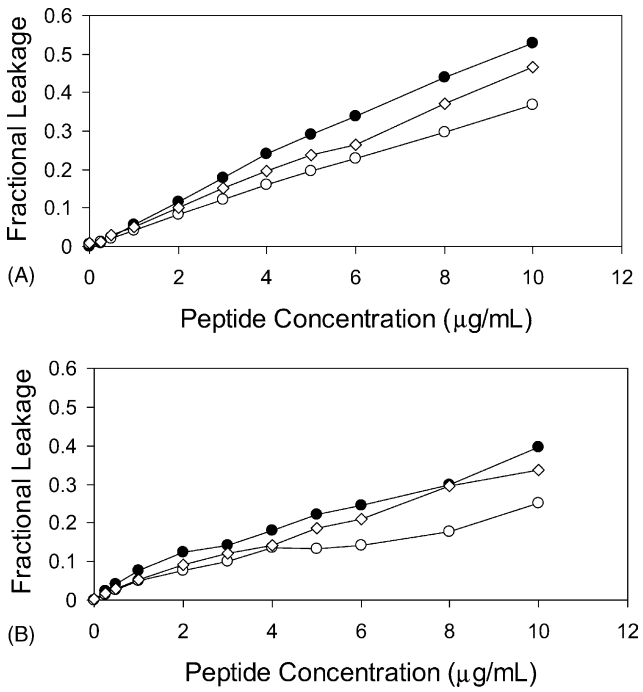

Fig. 9. Crp4 N-terminal variant induced leakage from LUV correlates with bactericidal activity. Vesicles composed of palmitoyl–oleoyl–phosphatidyl glycerol (POPG) (A) or of 80% POPG and 20% palmitoyl–oleoyl–phosphatidyl choline (POPG/POPC) (B) were prepared as described (Section 2). After exposure of vesicles to differing concentrations of Crp4 (●), (Gly1Arg)-Crp4 (◇), or (des-Gly)-Crp4 (○), fluorescence increases due to release of the fluorophore (ANTS) from quenched conditions inside the vesicle lumen. Fractional leakage is reported after 4 h (as calculated by the ratio of fluorescence increase relative to maximum fluorescence increase upon destroying the vesicles with the surfactant Triton X-100). The extents of leakage observed for the peptides examined are consistent with their respective bactericidal activities. Extent of leakage also depends on membrane composition, with membranes richer in anionic lipid more susceptible to peptide-induced perturbation.

Fluorescence requenching assays showed that all Crp4 peptides induced graded rather than all-or-none leakage. Thus, the Crp4 N-terminal variants induced leakage from LUV by a similar mechanism, and the slightly differing extents of leakage induced by the individual peptides were consistent with their modestly different bactericidal activities.

4. Discussion

In a previous report, certain cryptdin peptides purified from rinses of the mouse small intestinal lumen were found to have truncated N-termini and attenuated in vitro antimicrobial activities [24]. In bactericidal assays conducted by exposing bacteria to peptides in 10 mM PIPES (pH 7.4), (des-Gly)-Crp4 had markedly lower activity relative to Crp4. However, when microbicidal assays were modified by exposing the test bacteria to peptides in dilute (1%, v/v) microbiological media, the sensitivity and reproducibility of the assays improved, but (des-Gly)-Crp4 no longer had reduced activity relative to Crp4 (Figs. 3–5). It is not clear as to why the activity of (des-Gly)-Crp4 improved so drastically under the new assay conditions, but it is now clear that (des-Gly)-Crp4 and Crp4 have similar inherent bactericidal activities under the current assay conditions. Perhaps, as has been noted for certain neutrophil α-defensins, bacteria are more sensitive to membrane disruptive peptides when they are metabolically active [18]. Studies are being carried out to reconcile the differences in the (des-Gly)-Crp4 activities observed.

Relative to the striking attenuating effect of the N-terminal Asp on HNP-3 bactericidal activity [6], changes at the Crp4 peptide N-terminus produced very modest reduction or enhancement of Crp4 microbicidal activity. These differential effects of the N-terminus in the context of the HNP and Crp4 polypeptide structures suggest that the contribution of the N-terminal residue to the overall charge of the peptide influences activity more than N-terminal modification per se [8,41]. Because the Crp4 net charge (+8.5) is more than twice that of HNP-1 and -2 (+3), the unit charge reduction introduced by an electronegative N-terminal Asp residue in HNP-3 (+2) affects peptide charge, and possibly activity, more drastically than the comparable change in Crp4. It is also possible that N-terminal modifications different from those introduced here, i.e. Lys, Phe, or His, could alter Crp4 activity. On the other hand, studies of the single disulfide bonded peptide bactenecin have shown that increasing N- and C-terminal cationicity improved bactericidal peptide activity more than comparable changes in the loop formed by the disulfide bond [41]. As those authors suggested, addition of basic residues to the loop could affect peptide amphipathicity adversely, which reduced peptide activity despite increasing the overall charge of the peptide.

Although N-terminal changes at the Crp4 N-terminus induced only subtle changes in bactericidal activity, the differences between peptides corresponded directly to quantitative differences in their peptide–membrane interactions. Measurements of bacterial cell permeabilization kinetics (Fig. 6; Table 1), phospholipid dissociation constants measured by SPR (Fig. 7; Table 2), interactions with lipid/PDA mixed vesicles (Fig. 8), and induction of graded leakage from LUV of defined phospholipid composition (Fig. 9) showed that modified bactericidal activities by N-terminal substitution corresponded directly to quantitative differences in peptide–membrane interactions. For example, the (Gly1Arg)-Crp4 peptide has a reduced K_d for phospholipid bilayers, penetrated more deeply into the hydrophobic core of mixed vesicles, and induced LUV leakage more effectively (Fig. 9). Thus, even under conditions in which differences between the bactericidal activities of individual peptides are very modest, or perhaps especially so, quantitative assessment of membrane binding or membrane disruptive behavior of peptide variants correlates very well with biological activity.

Changes to N-terminal charge and hydrophobicity alter the microbicidal activity of natural HNP-1/3 more pro-

foundly than comparable changes in Crp4. Because the Cys1–Cys6 disulfide bond that exists in all α-defensins brings the N- and C-termini into proximity, changes at the N-terminus may be mitigated by the side chain composition of the amino acids that extend the peptide chain on the C-terminal side of Cys6. Crp4 and HNPs differ in this respect, because Crp4 has a Pro-Arg-Arg C-terminal extension, but HNP-1/3 terminates at Cys6 and has no C-terminal extension. Preliminary findings show that charge reversal at the Crp4 C-terminus and within the polypeptide chain diminish or eliminate bactericidal peptide activity and thus have more profound effects than corresponding N-terminal mutations (H. Tanabe et al., unpublished data). Perhaps, the lack of C-terminal amino acid side chains to interact with neighboring N-terminal residues accounts for the increased attenuating effect of N-terminal Asp on the biological activity of HNP-3 relative to Crp4. Introduction of (Asp1Lys)- or (Asp1Arg)-substitutions at the HNP-3 N-terminus and the addition of basic residues to the HNP-1 C-terminus should provide the means for testing this hypothesis.

Acknowledgments

Supported by NIH grants DK10184 (D.P.S.), AI22931 (M.E.S.), and DK44632 (A.J.O.) and the United States-Israel Binational Science Foundation (A.J.O., R.J.). R.J. is a member of the Ilse Katz Center for Meso- and Nanoscience and Technology, and J.E.C. acknowledges support from an NSF Fellowship. We thank Tim Cole, Vungie Hoang, and Khoa Nguyen for excellent technical assistance. Surface plasmon resonance studies were performed in the UCI Optical Biology Core Facility.

References

[1] Ayabe T, Satchell DP, Pesendorfer P, Tanabe H, Wilson CL, Hagen SJ, et al. Activation of Paneth cell alpha-defensins in mouse small intestine. J Biol Chem 2002;277:5219–28.
[2] Ayabe T, Satchell DP, Wilson CL, Parks WC, Selsted ME, Ouellette AJ. Secretion of microbicidal alpha-defensins by intestinal Paneth cells in response to bacteria. Nat Immunol 2000;1:113–8.
[3] Bechinger B. The structure, dynamics orientation of antimicrobial peptides in membranes by multidimensional solid-state NMR spectroscopy. Biochim Biophys Acta 1999;1462:157–83.
[4] Bevins CL, Martin-Porter E, Ganz T. Defensins innate host defence of the gastrointestinal tract. Gut 1999;45:911–5.
[5] Cooper MA, Try AC, Carroll J, Ellar DJ, Williams DH. Surface plasmon resonance analysis at a supported lipid monolayer. Biochim Biophys Acta 1998;1373:101–11.
[6] Ganz T, Selsted ME, Szklarek D, Harwig SS, Daher K, Bainton DF, et al. Defensins. Natural peptide antibiotics of human neutrophils. J Clin Invest 1985;76:1427–35.
[7] Geyer G. Lysozyme in Paneth cell secretions. Acta Histochem 1973;45:126–32.
[8] Hancock RE, Chapple DS. Peptide antibiotics. Antimicrob Agents Chemother 1999;43:1317–23.
[9] Hill CP, Yee J, Selsted ME, Eisenberg D. Crystal structure of defensin HNP-3, an amphiphilic dimer: mechanisms of membrane permeabilization. Science 1991;251:1481–5.
[10] Huang HW. Action of antimicrobial peptides: two-state model. Biochemistry 2000;39:8347–52.
[11] Hubbard JB, Silin V, Plant AL. Self assembly driven by hydrophobic interactions at alkanethiol monolayers: mechanisms of formation of hybrid bilayer membranes. Biophys Chem 1998;75:163–76.
[12] Kolusheva S, Boyer L, Jelinek R. A colorimetric assay for rapid screening of antimicrobial peptides. Nat Biotechnol 2000;18:225–7.
[13] Kolusheva S, Kafri R, Katz M, Jelinek R. Rapid colorimetric detection of antibody-epitope recognition at a biomimetic membrane interface. J Am Chem Soc 2001;123:417–22.
[14] Kolusheva S, Shahal T, Jelinek R. Peptide–membrane interactions studied by a new phospholipid/polydiacetylene colorimetric vesicle assay. Biochemistry 2000;39:15851–9.
[15] Lehrer RI, Barton A, Daher KA, Harwig SS, Ganz T, Selsted ME. Interaction of human defensins with Escherichia coli. Mechanism of bactericidal activity. J Clin Invest 1989;84:553–61.
[16] Lehrer RI, Barton A, Ganz T. Concurrent assessment of inner and outer membrane permeabilization and bacteriolysis in E. coli by multiple-wavelength spectrophotometry. J Immunol Methods 1988;108:153–8.
[17] Lehrer RI, Ganz T. Defensins of vertebrate animals. Curr Opin Immunol 2002;14:96–102.
[18] Lichtenstein AK, Ganz T, Nguyen TM, Selsted ME, Lehrer RI. Mechanism of target cytolysis by peptide defensins. Target cell metabolic activities, possibly involving endocytosis, are crucial for expression of cytotoxicity. J Immunol 1988;140:2686–94.
[19] Martinez-Bilbao M, Gaunt MT, Huber RE. E461H-beta-galactosidase (Escherichia coli): altered divalent metal specificity and slow but reversible metal inactivation. Biochemistry 1995;34:13437–42.
[20] Nyman KM, Ojala P, Laine VJ, Nevalainen TJ. Distribution of group II phospholipase A2 protein and mRNA in rat tissues. J Histochem Cytochem 2000;48:1469–78.
[21] Ouellette AJ, Bevins CL. Paneth cell defensins and innate immunity of the small bowel. Inflamm Bowel Dis 2001;7:43–50.
[22] Ouellette AJ, Darmoul D, Tran D, Huttner KM, Yuan J, Selsted ME. Peptide localization and gene structure of cryptdin 4, a differentially expressed mouse paneth cell alpha-defensin. Infect Immun 1999;67:6643–51.
[23] Ouellette AJ, Hsieh MM, Nosek MT, Cano-Gauci DF, Huttner KM, Buick RN, et al. Mouse Paneth cell defensins: primary structures and antibacterial activities of numerous cryptdin isoforms. Infect Immun 1994;62:5040–7.
[24] Ouellette AJ, Satchell DP, Hsieh MM, Hagen SJ, Selsted ME. Characterization of luminal Paneth cell alpha-defensins in mouse small intestine. Attenuated antimicrobial activities of peptides with truncated amino termini. J Biol Chem 2000;275:33969–73.
[25] Ouellette AJ, Selsted ME. Paneth cell defensins: endogenous peptide components of intestinal host defense. FASEB J 1996;10:1280–9.
[26] Peeters T, Vantrappen G. The Paneth cell: a source of intestinal lysozyme. Gut 1975;16:553–8.
[27] Porter EM, Bevins CL, Ghosh D, Ganz T. The multifaceted Paneth cell. Cell Mol Life Sci 2002;59:156–70.
[28] Satchell DP, Sheynis T, Shirafuji Y, Kolusheva S, Ouellette AJ, Jelinek R. Interactions of mouse Paneth cell alpha-defensins and alpha-defensin precursors with membranes: prosegment inhibition of peptide association with biomimetic membranes. J Biol Chem 2003;278:13838–46.
[29] Satoh Y. Effect of live and heat-killed bacteria on the secretory activity of Paneth cells in germ-free mice. Cell Tissue Res 1988;251:87–93.
[30] Satoh Y, Ishikawa K, Ono K, Vollrath L. Quantitative light microscopic observations on Paneth cells of germ-free and ex-germ-free Wistar rats. Digestion 1986;34:115–21.
[31] Selsted ME. Investigational approaches for studying the structures and biological functions of myeloid antimicrobial peptides. Genet Eng (NY) 1993;15:131–47.

[32] Selsted ME, Harwig SS. Determination of the disulfide array in the human defensin HNP-2. A covalently cyclized peptide. J Biol Chem 1989;264:4003–7.
[33] Selsted ME, Harwig SS. Purification, primary structure, and antimicrobial activities of a guinea pig neutrophil defensin. Infect Immun 1987;55:2281–6.
[34] Selsted ME, Harwig SS, Ganz T, Schilling JW, Lehrer RI. Primary structures of three human neutrophil defensins. J Clin Invest 1985;76:1436–9.
[35] Selsted ME, Miller SI, Henschen AH, Ouellette AJ. Enteric defensins: antibiotic peptide components of intestinal host defense. J Cell Biol 1992;118:929–36.
[36] Shirafuji Y, Tanabe H, Satchell DP, Henschen-Edman A, Wilson CL, Ouellette AJ. Structural determinants of procryptdin recognition and cleavage by matrix metalloproteinase-7. J Biol Chem 2003;278: 7910–9.
[37] Short ML, Nickel J, Schmitz A, Renkawitz R. Lysozyme gene expression and regulation. Exs 1996;75:243–57.
[38] Smolarsky M, Teitelbaum D, Sela M, Gitler C. A simple fluorescent method to determine complement-mediated liposome immune lysis. J Immunol Methods 1977;15:255–65.
[39] Vogt TC, Bechinger B. The interactions of histidine-containing amphipathic helical peptide antibiotics with lipid bilayers. The effects of charges and pH. J Biol Chem 1999;274:29115–21.
[40] Wilson CL, Ouellette AJ, Satchell DP, Ayabe T, Lopez-Boado YS, Stratman JL, et al. Regulation of intestinal alpha-defensin activation by the metalloproteinase matrilysin in innate host defense. Science 1999;286:113–7.
[41] Wu M, Hancock RE. Improved derivatives of bactenecin, a cyclic dodecameric antimicrobial cationic peptide. Antimicrob Agents Chemother 1999;43:1274–6.